Mon. Not. R. Astron. Soc. **000**, 1–?? ( ) Printed 4 November 2018 (MN LATEX style file v1.4)

J0041+3224: a new double-double radio galaxy

D.J. Saikia⋆, C. Konar and V.K. Kulkarni
National Centre for Radio Astrophysics, TIFR, Pune University Campus, Post Bag 3, Pune 411 007, India

Accepted. Received

ABSTRACT
We report the discovery of a double-double radio galaxy (DDRG), J0041+3224, with the Giant Metrewave Radio Telescope (GMRT) and subsequent high-frequency observations with the Very Large Array (VLA). The inner and outer doubles are aligned within ∼4° and are reasonably collinear with the parent optical galaxy. The outer double has a steeper radio spectrum compared with the inner one. Using an estimated redshift of 0.45, the projected linear sizes of the outer and inner doubles are 969 and 171 kpc respectively. The time scale of interruption of jet activity has been estimated to be ∼20 Myr, similar to other known DDRGs. We have compiled a sample of known DDRGs, and have re-examined the inverse correlation between the ratio of the luminosities of the outer to the inner double and the size of the inner double, l_{in}. Unlike the other DDRGs with $l_{in}\gtrsim$50 kpc, the inner double of J0041+3224 is marginally more luminous than the outer one. The two DDRGs with $l_{in}\lesssim$few kpc have a more luminous inner double than the outer one, possibly due to a higher efficiency of conversion of beam energy as the jets propagate through the dense interstellar medium. We have examined the symmetry parameters and find that the inner doubles appear to be more asymmetric in both its armlength and flux density ratios compared with the outer doubles, although they appear marginally more collinear with the core than the outer double. We discuss briefly possible implications of these trends.

Key words: galaxies: active – galaxies: nuclei – galaxies: individual: J0041+3224 – radio continuum: galaxies

1 INTRODUCTION

One of the important issues concerning galaxies is the duration of their active galactic nuclei (AGN) phase and whether such periods of activity are episodic. In the currently widely accepted paradigm, activity is believed to be intimately related to the 'feeding' of a supermassive black hole whose mass ranges from ∼10^6 to 10^{10} $M_\odot$. Such an active phase may be recurrent with an average total timescale of the active phases being ∼10^8 to 10^9 yr (cf. Marconi et al. 2004, and references therein).

Of the galaxies harbouring an AGN, a small fraction appears to be luminous at radio wavelengths. For example, in the SDSS (Sloan Digital Sky Survey) quasars, ∼8 per cent of the bright ones (i <18.5) are radio loud in the sense that the ratio of radio to X-ray flux exceeds unity (Ivezić et al. 2002, 2004). Although what physical conditions determine loudness still remains unclear, Nipoti, Blundell & Binney (2005) have suggested recently that this may simply be a function of the epoch at which the source is observed.

For the radio-loud objects, an interesting way of probing their history is via the structural and spectral information of the lobes of extended radio emission. Such studies have been used to probe sources which exhibit precession or changes in the ejection axis, effects of motion of the parent galaxy, backflows from hotspots as well as X-shaped sources and major interruptions of jet activity. For example, the radio galaxy 3C388 exhibits two distinct regions of emission separated by a jump in spectral index, which has been interpreted to be due to two different epochs of jet activity (Burns, Schwendeman & White 1983; Roettiger et al. 1994). A ridge of emission, reminescent of a jet but displaced towards the south of the nucleus in the radio galaxy 3C338 could also be due to intermittent jet activity (Burns, Schwendeman & White 1983). Other suggestions of distinct epochs of jet activity based on spectral index studies include Her A, where the bright inner regions have flatter spectra with a sharp boundary delineating it from the more extended lobe emission, especially in the western lobe (Gizani & Leahy 2003), and 3C310 where the inner components B and D have substanially flatter spectra than the surrounding lobes (van Breugel & Fomalont 1984; Leahy et al. 1986). An interesting example of different epochs of jet activity is the well-studied radio galaxy Cen A, where in addition to

⋆ E-mail: djs@ncra.tifr.res.in

the diffuse outer lobes there are the more compact inner lobes and a northern middle lobe or NML (Burns, Feigelson & Schreier 1983; Clarke, Burns & Norman 1992; Junkes et al. 1993). Morganti et al. (1999) have detected a large-scale jet connecting the northern lobe of the inner double and the NML, and have suggested that the formation of the NML may be due to a 'bursting bubble' in which plasma accumulated in the inner lobe bursts out through a nozzle. A lobe of emission on only one side of the nuclear region has also been seen in the Gigahertz Peaked Spectrum radio source B0108+388, and has been suggested to be a relic of a previous cycle of jet activity (Baum et al. 1990). However, the one-sidedness of the emission is puzzling (cf. Stanghellini et al. 2005), and it would be interesting to examine whether a 'bursting bubble' model may also be applicable in such cases.

One of the more striking examples of episodic jet activity is when a new pair of radio lobes is seen closer to the nucleus before the 'old' and more distant radio lobes have faded. Such sources have been christened as 'double-double' radio galaxies (DDRGs) by Schoenmakers et al. (2000, hereinafter referred to as S2000). They proposed a relatively general definition of a DDRG as a double-double radio galaxy consisting of a pair of double radio sources with a common centre. S2000 also suggested that the two lobes of the inner double should have an edge-brightened radio morphology to distinguish it from knots in a jet. In such sources the newly-formed jets propagate outwards through the cocoon formed by the earlier cycle of activity rather than the general intergalactic or intracluster medium, after traversing through the interstellar medium of the host galaxy. Approximately a dozen or so of such DDRGs are known in the literature (S2000; Saripalli et al. 2002, 2003; Schilizzi et al. 2001; Marecki et al. 2003). We have included objects such as 3C236 (Schilizzi et al. 2001) and J1247+6723 (Marecki et al. 2003) in this category since the principal difference is only in the size of the inner double which is $\lesssim$few kpc. It is important to identify more DDRGs not only for understanding episodic jet activity and examining their time scales, but also for studying the propagation of jets in different media. For example, to explain the edge-brightened hotspots in the inner doubles of the DDRGs, Kaiser, Schoenmakers & Röttgering (2000) have suggested that warm (T$\sim$10^{4}K) clouds of gas in the intergalactic medium are dispersed over the cocoon volume by surface instabilities induced by the passage of the cocoon material.

In this paper we report the discovery of a new DDRG, J0041+3224, identified from observations made with the Giant Metrewave Radio Telescope (GMRT) of candidate DDRGs from the B2 sample (Padrielli, Kapahi & Katgert-Merkelijn 1981; Saikia et al. 2002). Our candidates were identified by comparing the large- and smaller-scale images made either by us or those available in the literature. J0041+3224 was reported by Padrielli et al. (1981) to be double-lobed with an angular size of 32 arcsec. They identified the radio source to be associated with a galaxy with a visual magnitude of 20.0 and located at RA $00^h\ 41^m\ 46.^s11$, Dec: $+32^\circ\ 24'\ 53.''8$ in J2000 co-ordinates. There is no measured redshift of the galaxy. From the V magnitude−redshift diagram (Guiderdoni & Rocca-Volmerange 1987) we estimate the redshift to be $\sim$0.45 and use this value for this paper.

Table 1. Observing log

Telescope	Array Conf.	Obs. Freq. MHz	Obs. Date
GMRT		617	2002 Jul 27
GMRT		1287	2002 Jun 21
VLA	C	1400	2002 Nov 28
VLA	C	4860	2002 Nov 28
VLA	C	8460	2002 Nov 28

2 OBSERVATIONS AND ANALYSES

The GMRT consists of thirty 45-m antennas in an approximate 'Y' shape similar to the VLA but with each antenna in a fixed position. Twelve antennas are randomly placed within a central 1 km by 1 km square (the "Central Square") and the remainder form the irregularly shaped Y (6 on each arm) over a total extent of about 25 km. Further details about the array can be found at the GMRT website at `http://www.gmrt.ncra.tifr.res.in`. The observations were made in the standard fashion, with each source observation interspersed with observations of the phase calibrator. The flux densities are on the Baars et al. (1977) scale.

The observations with the VLA were made in the snapshot mode in the L, C and X bands. The flux densities are again on the Baars et al. (1977) scale. All the data were calibrated and analysed in the standard way using the NRAO `AIPS` package.

The observing log for both the GMRT and the VLA observations are listed in Table 1 which is arranged as follows. Columns 1 and 2 show the name of the telescope, and the array configuration for the VLA observations; column 3 shows the frequency of the observations, while the dates of the observations are listed in column 4.

3 OBSERVATIONAL RESULTS

All the images of the source are presented in Figs. 1, 2 and 4, while the observational parameters and some of the observed properties are presented in Table 2, which is arranged as follows. Column 1: frequency of observations in units of MHz, with the letter G or V representing either GMRT or VLA observations; columns 2−4: the major and minor axes of the restoring beam in arcsec and its position angle (PA) in degrees; column 5: the rms noise in units of mJy/beam; column 6: the integrated flux density of the source in mJy estimated by specifying an area around the source; column 7, 10, 13 and 16: component designation where W1 and E1 indicate the western and eastern components of the outer double, W2 and E2 the western and eastern components of the inner double (Fig. 1, lower panel); columns 8 and 9, 11 and 12, 14 and 15, 17 and 18: the peak and total flux densities of the components in units of mJy/beam and mJy respectively. The flux densities have been estimated by specifying an area around each component.

The low-resolution NVSS image with an angular resolution of 45 arcsec (Fig. 1, upper panel) shows a more compact western component and a well-resolved eastern one. The VLA C-array image at 1400 MHz (Fig. 1, lower panel) with an angular resolution of $\sim$13.6 arcsec shows the source

Table 2. The observational parameters and observed properties of the sources

Freq.	Beam size			rms	S_I	Cp	S_p	S_t	Cp	S_p	S_t	Cp	S_p	S_t	Cp	S_p	S_t
MHz	$''$	$''$	$^\circ$	mJy /b	mJy		mJy /b	mJy		mJy /b	mJy		mJy /b	mJy		mJy /b	mJy
(1)	(2)	(3)	(4)	(5)	(6)	(7)	(8)	(9)	(10)	(11)	(12)	(13)	(14)	(15)	(16)	(17)	(18)
G617	6.5	4.8	165	0.49	2211	W1	98	542	W2	274	314	E2	567	691	E1	135	598
G1287	2.6	2.3	25	0.20	1104	W1	12	233	W2	92	145	E2	231	373	E1	13	227
V1400	45.0	45.0		0.51	967												
V1400	14.7	12.6	11	0.16	940	W1	108	207	W2	139	148	E2	338	377	E1	117	202
V4860	4.0	3.7	13	0.03	298	W1	7.4	50	W2	42	52	E2	126	154	E1	6.0	37
V8460	2.4	2.3	19	0.01	153	W1	1.4	12	W2	21	32	E2	75	100	E1	0.9	7.6

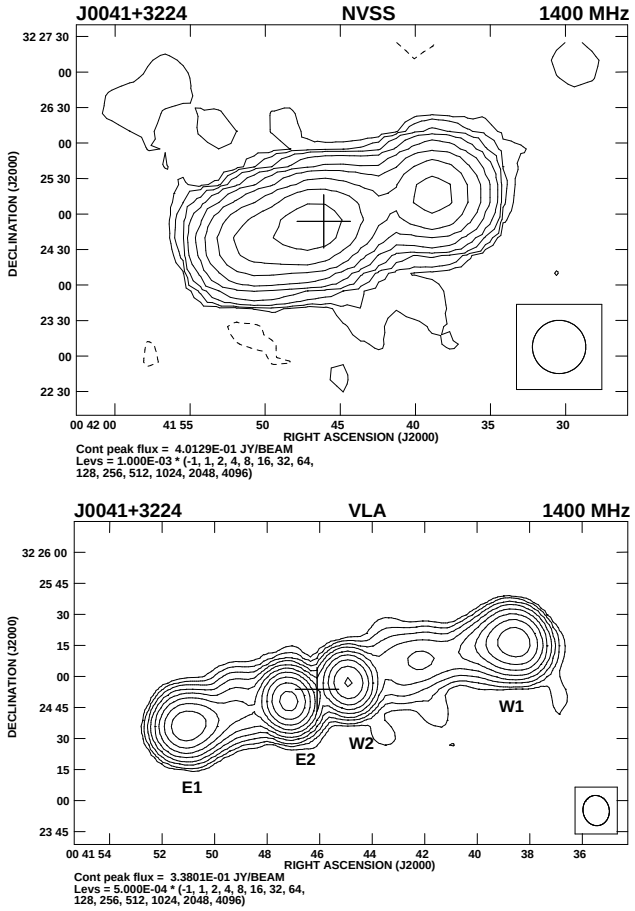

Figure 1. The NVSS image of J0041+3224 with an angular resolution of 45 arcsec (upper panel) and the VLA C-array image at 1400 MHz with an angular resolution of ∼13.6 arcsec. In all the images presented in this paper the restoring beam is indicated by an ellipse, and the + sign indicates the position of the optical galaxy.

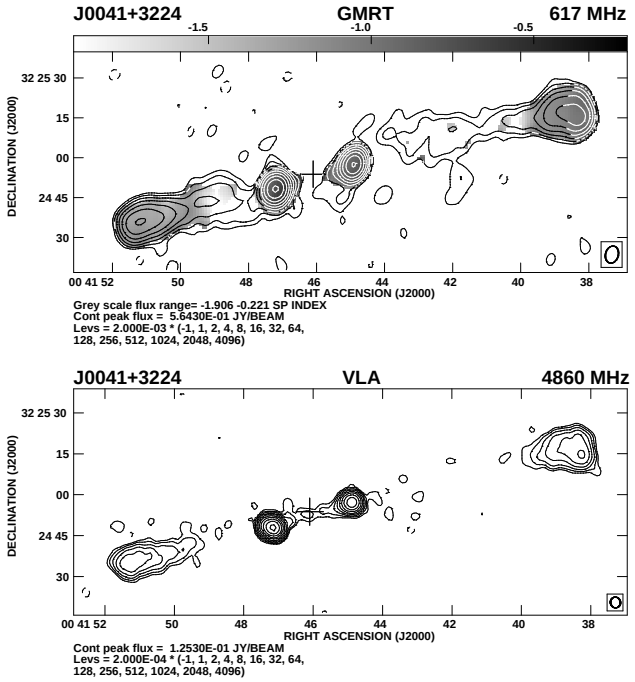

Figure 2. The GMRT image of J0041+3224 at 617 MHz with an angular resolution of ∼5.6 arcsec (upper panel) and the VLA C-array image at 4860 MHz with an angular resolution of ∼3.8 arcsec (lower panel). The spectral index image obtained by smoothing the 4860-MHz image to that of the 617-MHz one is shown superimposed on the 617-MHz image in gray scale.

could be a DDRG with the eastern NVSS component being resolved into the inner double and the eastern component of the outer double. The optical galaxy lies between the components of the inner double-lobed source. The PAs of the outer and inner doubles are 104° and 108° respectively, showing the close alignment seen in a number of other DDRGs (cf. S2000).

In Fig. 2 we show the GMRT image at 617 MHz with an angular resolution of ∼5.6 arcsec and the VLA image at 4860 MHz with an angular resolution of ∼3.8 arcsec. These images show the lobes of the inner double to be well separated and lying on opposite sides of the parent optical galaxy. Weak tails of emission towards the optical galaxy are visible from both the components of the inner double in the VLA image. These tails merge to form a weak bridge of emission between the two components. The spectral index image between 617 and 4860 MHz obtained by smoothing the VLA image at 4860 MHz to that of the GMRT one is shown superimposed on the GMRT image, while the spectral index slices for the western and eastern lobes of the outer double are shown in Fig. 3. The spectral index image has been made for regions which are at least 5 times the rms value in both images. The spectral index, α, defined as $S \propto \nu^{\alpha}$, varies from -0.8 to -1.5 in the western lobe, while for the

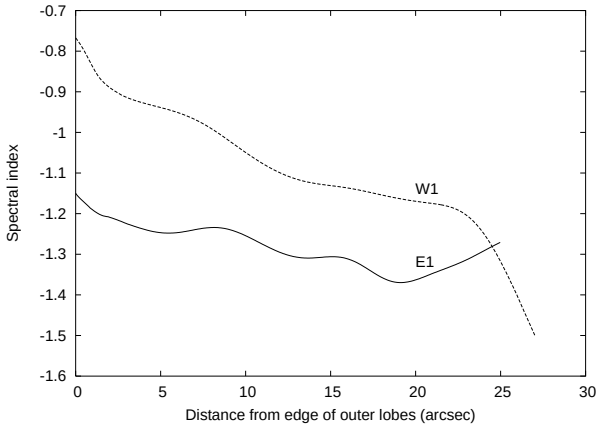

Figure 3. Slices of spectral index between 617 and 4860 MHz for the western and eastern components of the outer double.

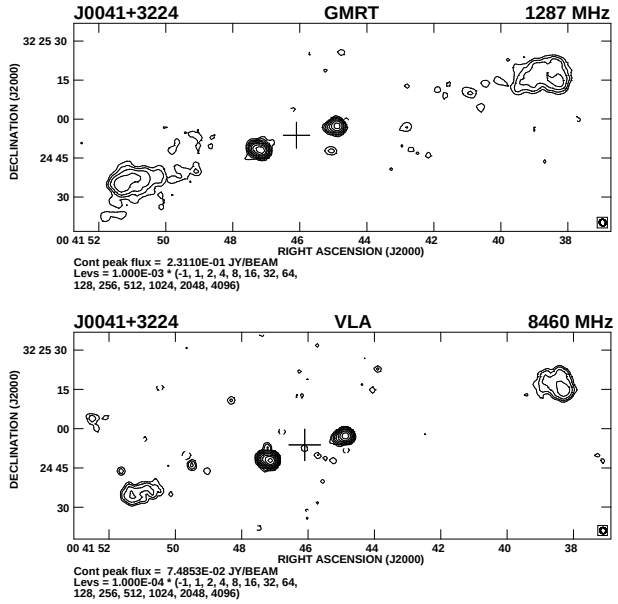

Figure 4. The GMRT image of J0041+3224 at 1287 MHz with an angular resolution of ∼2.7 arcsec (upper panel) and the VLA C-array image at 8460 MHz with an angular resolution of ∼2.4 arcsec (lower panel).

eastern lobe it varies from −1.2 to −1.4. The typical error in the spectral index is ∼0.1 assuming an error of 5 per cent in the measured flux density. Using the formalism of Myers & Spangler (1985), the steepening in the western lobe (W1), which has an equipartition magnetic field (e.g. Miley 1980) of 0.75 nT, corresponds to a spectral age $\gtrsim 6\times10^6$ yr. The eastern component (E1) has a steeper spectrum but its spectral variation is small.

Our higher-resolution images with the GMRT at 1287 MHz and with the VLA at 8460 MHz with angular resolutions of ∼2.7 and 2.4 arcsec respectively are shown in Fig. 4. The inner components are resolved with angular sizes of 1.8×1.0 arcsec^2 along a PA of 105° for the western component and 2.8×0.8 arcsec^2 along a PA of 74° for the eastern one. These have been estimated from the lower-frequency GMRT image. The values are similar using the VLA 8460-

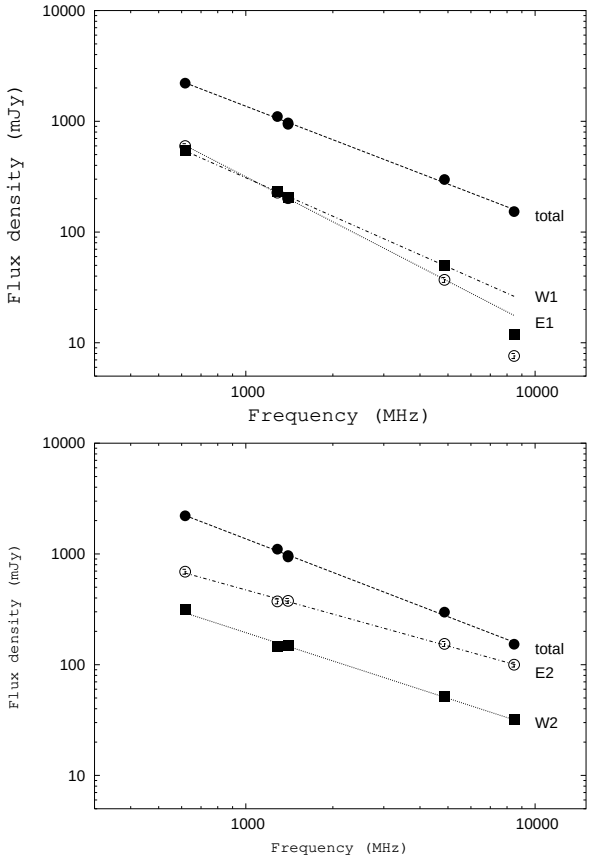

Figure 5. The spectra of the western and eastern components of the outer double (upper panel) and the inner double (lower panel). The integrated spectrum is shown in both the panels.

MHz image of similar resolution. The western component of the inner double is extended towards the direction of the optical object while the eastern component is extended at about 34° to the axis of the source. This is not surprising given the complexity of the structures of hotspots and emission in their vicinity (cf. Black et al. 1992; Leahy et al. 1997; Hardcastle et al. 1997).

There is a possible detection of a radio core in our data. The peak of emission in the weak bridge seen in VLA image at 4860 MHz, has a peak flux density of 0.57 mJy/beam and is within ∼1 arcsec of the optical position. If this is indeed the radio core, its flux density is likely to be lower since this value could be contaminated by emission from the bridge. The peak flux density near the optical position in the 8460-MHz image is 0.2 mJy/beam and is at the same location as the peak of emission in the 4860-MHz image. This feature could be the radio core, although it requires confirmation.

The integrated spectra of the entire source and of the individual components along with the linear least-square fits to the spectra using our measurements are shown in Fig. 5. The spectra of the components for the outer and inner doubles are shown in the upper and lower panels respectively, while the integrated spectrum is shown in both the panels. The spectral index of the entire source is −1.01±0.02, while that of the western and eastern components of the outer double are −1.15±0.01 and −1.35±0.01 respectively. The corresponding values for the inner double are −0.85±0.03

Table 3. The sample of DDRGs

Source	Opt. Id.	Red-shift	l_{in} kpc	l_o kpc	Cmp.	$R_{\theta(in)}$	$R_{\theta(o)}$	$R_{s(in)}$	$R_{s(o)}$	Δ_{in} °	Δ_o °	P_{in} W/Hz	P_o W/Hz	Ref.
(1)	(2)	(3)	(4)	(5)	(6)	(7)	(8)	(9)	(10)	(11)	(12)	(13)	(14)	(15)
J0041+3224	G	0.45	171	969	W/E	1.17	1.49	0.39	1.02	0	3	26.55	26.52	1
J0116−4722	G	0.146	460	1447	N/S	1.06	1.42			4	20	25.14	26.16	2
J0921+4538	G	0.174	69	433	S/N	3.61	0.96	29.00	1.03	1	11	24.86	26.82	3,4,5
J0929+4146	G	0.365	652	1875	N/S	1.55	1.06	1.12	0.77	3	5	25.42	25.64	6
J1006+3454	G	0.101	1.7	4249	W/E	3.15	0.61	0.38	1.35	15	2	25.86	25.63	7,8,9
J1158+2621	G	0.112	138	483	N/S	1.23	0.99	1.74	1.13	0	1	25.31	25.48	10
J1242+3838	G	0.300	251	602	N/S	1.74	0.90	2.00	1.59	1	3	24.32	24.84	6
J1247+6723	G	0.107	0.014	1195								24.87	24.55	11,12
J1453+3308	G	0.249	159	1297	S/N	1.06	1.34	0.16	0.49	3	11	24.77	25.90	6
J1548−3216	G	0.108	313	961	S/N	1.24	1.07			4	4	24.34	25.69	13
J1835+6204	G	0.519	369	1379	N/S	1.03	1.02	0.89	1.89	1	0	26.27	26.81	6
J2223−0206	G	0.056	130	612	S/N	1.77	0.95	2.66	1.51	2	6	23.61	25.58	14,15

1: Present paper; 2: Saripalli, Subrahmanyan & Udaya Shankar 2002; 3: Perley et al. 1980; 4: Bridle, Perley & Henriksen 1986; 5: Clarke et al. 1992; 6: Schoenmakers et al. 2000; 7: Willis, Strom & Wilson 1974; 8: Strom & Willis 1980; 9: Schilizzi et al. 2001; 10: Owen & Ledlow 1997; 11: Marecki et al. 2003; 12: Bondi et al. 2004; 13: Saripalli, Subrahmanyan & Udaya Shankar 2003; 14: Kronberg, Wielebinski & Graham 1986; 15: Leahy et al. 1997.

and -0.73 ± 0.02 respectively. For the outer double the fits have been made by excluding the flux densities at 8460 MHz. There is some evidence of spectral steepening above 4860 MHz, but we need to make lower resolution images at higher frequencies to estimate any missing flux density, and hence the degree of spectral steepening.

4 DISCUSSION AND RESULTS

The images of J0041+3224 suggest that there have been two main episodes of activity, represented by the outer and inner double-lobed structures which are well aligned and roughly collinear with the parent optical galaxy. The lobes of the outer double are separated by 169 arcsec, corresponding to 969 kpc, while the inner double has a separation of 29.9 arcsec, corresponding to 171 kpc ($H_\circ$=71 km s^{-1} Mpc^{-1}, Ω_m=0.27, Ω_Λ=0.73, Spergel et al. 2003). The radio luminosities of the outer and inner doubles at an emitted frequency of 1.4 GHz are 3.3 and 3.6×10^{26} W Hz^{-1} respectively, both well above the FRI-FRII divide, and consistent with their observed structures.

The lobes of the outer double represent an earlier period of activity. These lobes have steeper spectral indices than the inner lobes (Fig. 5), possible evidence of spectral steepening and no prominent hotspots, while the inner lobes which represent ongoing activity are dominated by bright hotspots. The ratio of the average peak brightness of the inner double to the outer double in our VLA 8460-MHz images which have angular resolutions of $\sim$2.4 arcsec is $\gtrsim$40. The angular resolution in these images corresponds to a linear size of $\sim$14 kpc, which is within the range for sizes of hotspots for sources of similar linear size (cf. Leahy et al. 1997; Jeyakumar & Saikia 2000).

When the jet is interrupted and energy supply to the outer hotspots ceases, the channel will collapse due to the loss of pressure which is provided by the jet material (e.g. Kaiser & Alexander 1997). This implies that the restarted jet will have to drill out a new channel. However, unlike the earlier jet which propagates through the interstellar and intracluster or intergalactic medium, the restarted jet propagates into the relic synchrotron plasma created by the earlier cycle of activity after ploughing its way through the interstellar medium of the host galaxy. The density of the synchrotron plasma is expected to be significantly smaller than the intergalactic medium (Clarke & Burns 1991; Cioffi & Blondin 1992; Loken et al. 1992), by up to a factor of 100, unless there is significant entrainment (Kaiser et al. 2000). Without entrainment, only weak shocks are expected as the jet propagates through the synchrotron plasma. In this case, the jets move ballistically without generating prominent hotspots and cocoons. This appears to be the case, for example, in J1548−3216 (Saripalli et al. 2003). In the case of J0041+3224, the detection of prominent hotspots in the inner lobes suggest the existence of significant thermal material, as has been suggested by Kaiser et al. (2000) to explain the formation of hotspots in their sample of DDRGs.

An estimate of the time scale of interruption and restarting of jet activity could provide insights in determining the cause of the interruption. A weak constraint on the upper limit to the time scale of interruption can be provided by the fact that the outer lobes are still visible. For a sample of 'relic' radio sources, Komissarov & Gubanov (1994) have estimated the time scales for the source to fade away to be a few times 10^7 yr, which is comparable to the kinematic age of the source itself. For example, for a velocity of advancement of $\sim$0.1c, the kinematic age of the outer double is $\sim3.2\times10^7$ yr. One might expect the jets of the inner double to have higher velocities of advancement if it encounters only the low-density synchrotron plasma (e.g. Clarke & Burns 1991). However, the formation of strong hotspots suggests it is encountering a dense medium, possibly due to entrainment, and we assume the velocities to be similar. For a projected linear size of 171 kpc for the inner double, the age of the inner double is 5.6×10^6 yr. This leaves us with a time scale of $\sim$20 Myr between stopping and restarting of the jet.

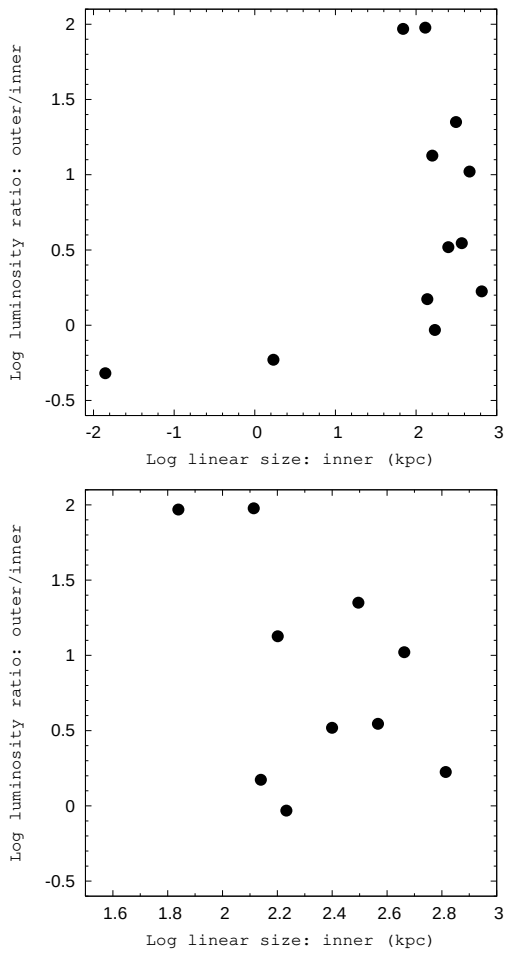

Figure 6. Luminosity ratio of the outer double to that of the inner double, $P_{o:in}$, at an emitted frequency of 1400 MHz is plotted against l_{in}, the projected linear size of the inner double (upper panel). The same plot for those with $l_{in}\gtrsim$50 kpc is shown in the lower panel.

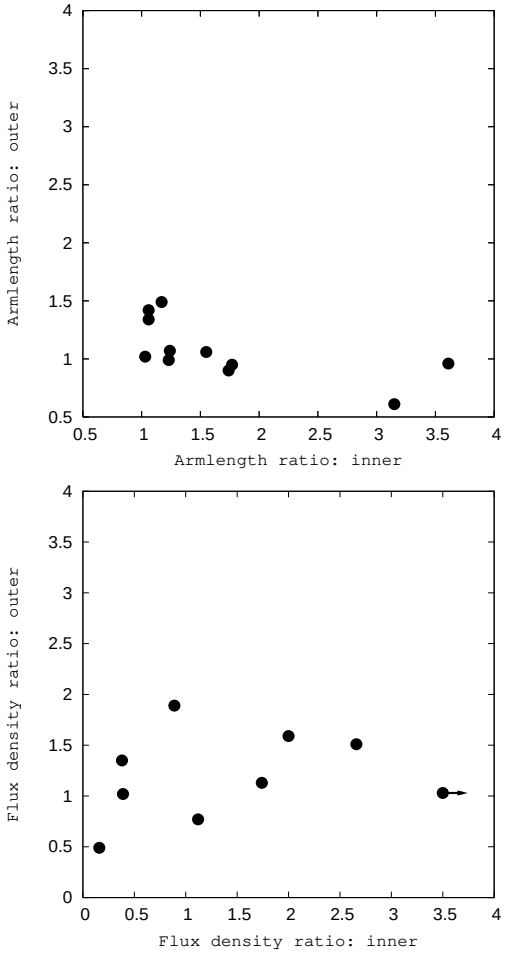

Figure 7. The armlength (upper panel) and flux density (lower panel) ratios of the inner doubles are plotted against the corresponding values for the outer doubles for the sample of DDRGs. The sense of direction of the components is described in Section 4.1 and listed in Table 3.

4.1 Luminosities of outer and inner doubles

The luminosities of the outer and inner doubles of J0041+3224 are comparable, the ratio, $P_{o:in}$, being ∼0.93 at an emitted frequency of 1400 MHz. This is unlike the sample of DDRGs compiled by S2000 where the outer lobes were always found to be more luminous than the inner ones. S2000 also noted that $P_{o:in}$ decreases with, l_{in}, the separation of the inner double. We have re-examined this relationship by enlarging the sample of DDRGs to include those which have been reported more recently, as well as those where the inner doubles are of subgalactic dimesnions, as in J1006+3454 (3C236) and J1247+6723. Candidate DDRGs mentioned by S2000 such as 4C12.03, 3C16 (Leahy & Perley 1991) and 3C424 (Black et al. 1992) which require further observations to clarify their structures have not been presently included in the sample. The sample is listed in Table 3 and is arranged as follows. Column 1: source name; column 2: optical identification; column 3: redshift; columns 4 and 5: projected linear size of the inner and outer double-lobed source in kpc; columns 6: the locations of the components farther/closer from the core for the inner double. The symmetry parameters in columns 7 to 10 are all in the same sense as in column 6. Columns 7 and 8: the arm-length or separation ratio for the inner and outer doubles; columns 9 and 10: flux density ratios for the inner and outer doubles; columns 11 and 12: the misalignment angles, defined to be the supplement of the angle formed at the core by the hotspots or peaks of emission for the inner and outer lobes; columns 13 and 14: log of radio luminosity at an emitted frequency of 1.4 GHz for the inner and outer doubles; column 15: references for the radio structure.

In Fig. 6, we plot the ratio of the luminosities of the outer to the inner doubles against the separation of the inner double. Both the sources with $l_{in}\lesssim$1 kpc have a more luminous inner double than the outer one, unlike all the sources in the sample of S2000 where $l_{in}\gtrsim$50 kpc. For comparison with the plot by S2000 we have also plotted the sources with $l_{in}\gtrsim$50 kpc separately. It is possible that in the early phase of the evolution of the inner double, where it is ploughing its way through the dense interstellar medium, conversion of beam energy into radio emission may be more efficient. This could lead to a ratio of the luminosities of the outer to the inner doubles being significantly less than unity. As

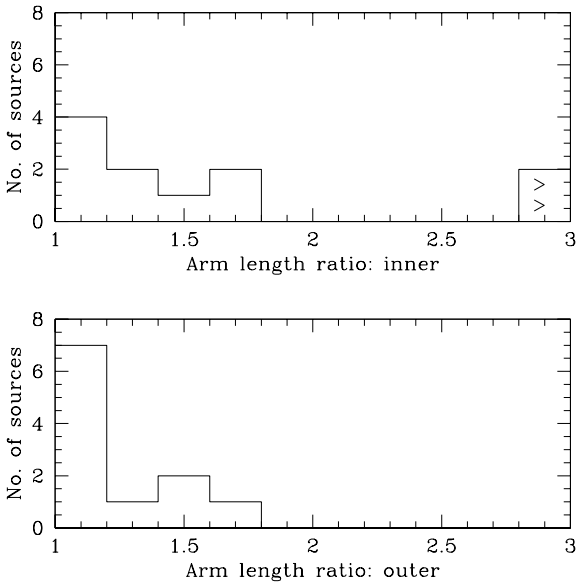

Figure 8. The distributions of the armlength ratios for the inner and outer doubles, defined to be $\geq$1. The > sign indicates a value larger than the range plotted in the histogram.

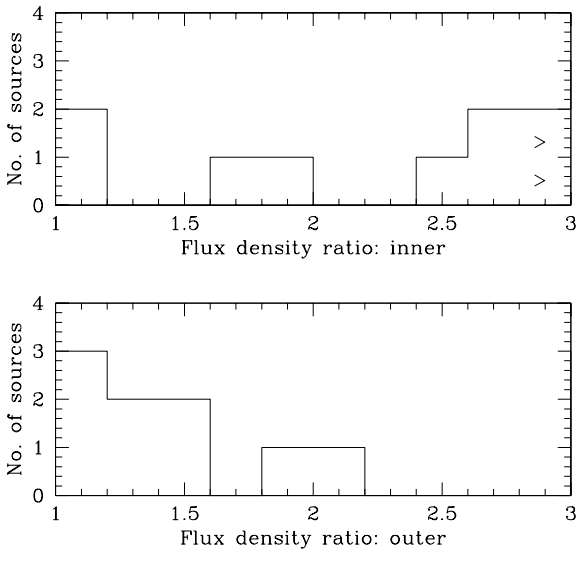

Figure 9. The distributions of the flux density ratios for the inner and outer doubles, defined to be $\geq$1. The > sign indicates a value larger than the range plotted in the histogram.

the source expands and traverses through a more tenuous medium, the ratio could increase with size before approaching values of unity for large values of l_{in} (cf. S2000). We have re-examined the inverse correlation suggested by S2000 considering only those objects with $l_{in}\gtrsim$50 kpc and find the correlation to have a Spearman rank correlation coefficient of -0.37, compared with a value of -0.57 for the objects in the sample of S2000.

4.2 Symmetry parameters

A comparison of the symmetry parameters of the inner and outer doubles might provide insights into the environments in which the jets are propagating as well as any possible intrinsic asymmetries in the jets themselves. In the case of the restarted jets advancing into synchrotron relics from earlier epochs of activity, one might expect similar environments and hence more symmetric structures for the inner doubles.

In Fig. 7, we show the armlength and flux density ratios of the outer doubles plotted against the corresponding values for the inner doubles for the sample of DDRGs. The sense of direction of the components is described in Section 4.1 and listed in Table 3. It appears that the inner doubles tend to be more asymmetric in both its armlength and flux density ratios compared with the outer doubles. The distributions for the armlength ratios, now defined to be always >1, show that the median values are ∼1.3 and 1.1 for the inner and outer doubles respectively (Fig. 8). A Kolmogorov–Smirnov test shows the distributions to be different at a significance level of 0.30. A similar trend is also seen in the distributions of the flux density ratios, again defined to be always >1, for the inner and outer lobes. The median values are ∼2.5 and 1.4 respectively (Fig. 9), and the two distributions are different at a significance level of 0.10. It is also worth noting (see Table 3) that the asymmetries in the inner and outer doubles are not in the same sense. Although these

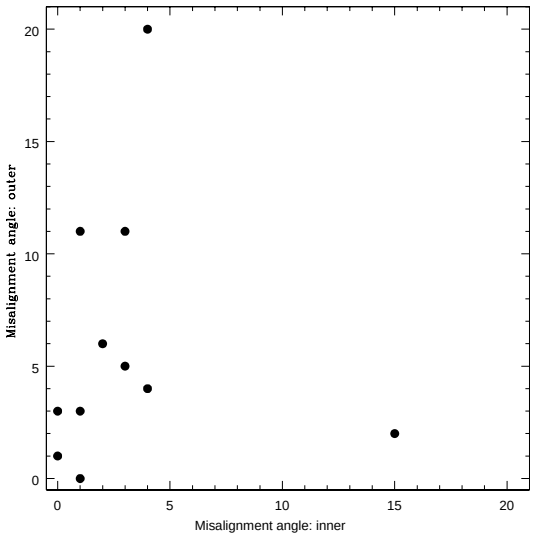

Figure 10. The misalignment angle of the outer double in degrees is plotted against the corresponding value for the inner double.

trends need to be confirmed with larger samples, they are possibly a reflection of different environments, possibly due to different degrees of entrainment in the cocoons on opposite sides coupled with effects of relativistic beaming and any intrinsic jet asymmetries. For example, in the case of J0921+4538, the armlength ratio of 3.61 for the inner double can be understood in the relativistic beaming framework if the velocity is ∼0.8c for an inclination angle of 45°, the dividing line between radio galaxies and quasars in the unified scheme (Barthel 1989). This is also in reasonable agreement with the flux density ratio of 29. However, in the case of the inner double of J1006+3454, where the armlength ra-

tio is 3.15, the flux density ratio is 0.38, suggesting intrinsic asymmetries.

The median values of the misalignment angle of the inner and outer doubles are ∼2 and 4° respectively (Fig. 10). A Kolmogorov–Smirnov test shows the distributions to be different at a significance level of 0.3. This could arise due to the lobes of the outer double responding to either large-scale density gradients or motion of the parent optical galaxy during the two cycles of jet activity.

5 CONCLUDING REMARKS

We have reported the discovery of a new double-double radio galaxy, J0041+3224, with the GMRT and subsequent observations with the VLA. Using an estimated redshift of 0.45, the projected linear size of the outer double is 969 kpc. Large linear sizes are characteristic of most of the known DDRGs. The lobes of the outer double have steeper spectral indices compared with those of the inner double. The kinematic age of the outer double is $\sim 3\times10^7$ yr, while the time scale of interruption of jet activity is ∼20 Myr. Unlike most DDRGs with $l_{in}\gtrsim$50 kpc, the inner double of J0041+3224 is marginally more luminous than the outer one. S2000 reported an inverse correlation between the ratio of the luminosities of the outer and inner doubles, $P_{o:in}$, and l_{in}. For their sample of DDRGs the luminosity ratio, $P_{o:in}$, is as high as ∼100 for l_{in}∼50 kpc and approaches unity when l_{in} approaches values close to a Mpc, the ratio being always >1. Considering the more compact inner doubles with $l_{in} \lesssim$ few kpc, namely J1006+3454 (3C236) and J1247+6723, the inner doubles are significantly more luminous than the outer ones. This suggests that in the early phase of the evolution of the inner double, where it is ploughing its way through the dense interstellar medium, conversion of beam energy into radio emission may be more efficient. In this case, the ratio of the luminosity of the outer to the inner double could increase with size before decreasing and approaching a value of about unity when l_{in} approaches ∼1 Mpc. We have re-examined the inverse correlation for sources with $l_{in}\gtrsim$50 kpc with the addition of a few more sources and find the correlation to have a rank correlation co-efficient of −0.37, compared with a value of −0.57 for the objects in the sample of S2000.

We have compared the symmetry parameters of the inner and outer doubles and find that the inner doubles appear to be more asymmetric in both its armlength and flux density ratios compared with the outer doubles. Also, the asymmetries in the inner and outer doubles are not in the same sense. Although these trends need to be confirmed with larger samples, they are possibly a reflection of different environments due to different degrees of entrainment in the cocoons on opposite sides, coupled with any intrinsic jet asymmetries and effects of relativistic motion. However, the inner doubles appear marginally more collinear with the radio core than the outer doubles. This could arise due to the lobes of the outer double responding to large-scale density gradients, or motion of the parent optical galaxy during the two cycles of nuclear activity.

ACKNOWLEDGMENTS

We thank our colleagues for useful discussions, an anonymous referee, Dave Green and Paul Wiita for their comments on the manuscript and the telescope operators for their help with the observations. The Giant Metrewave Radio Telescope is a national facility operated by the National Centre for Radio Astrophysics of the Tata Institute of Fundamental Research. The National Radio Astronomy Observatory is a facility of the National Science Foundation operated under co-operative agreement by Associated Universities Inc. This research has made use of the NASA/IPAC extragalactic database (NED) which is operated by the Jet Propulsion Laboratory, Caltech, under contract with the National Aeronautics and Space Administration.

REFERENCES

Baars J.W.M., Genzel R., Pauliny-Toth I.I.K., Witzel A. 1977, A&A, 61, 99
Barthel P.D., 1989, ApJ, 336, 606
Baum S.A., O'Dea C.P., de Bruyn A.G., Murphy D.W., 1990, A&A, 232, 19
Black A.R.S., Baum S.A., Leahy J.P., Perley R.A., Riley J.M., Scheuer P.A.G., 1992, MNRAS, 256, 186
Bondi M., Marchã, M.J.M., Polatidis A., Dallacasa D., Stanghellini C., Antón S., 2004, MNRAS, 352, 112
Bridle A.H., Perley R.A., Henriksen R.N., 1986, AJ, 92, 534
Burns J.O., Feigelson E.D., Schreier E.J., 1983, ApJ, 273, 128
Burns J.O., Schwendeman E., White R.A., 1983, ApJ, 271, 575
Cioffi D.F., Blondin J.M., 1992, ApJ, 392, 458
Clarke D.A., Burns J.O., 1991, ApJ, 369, 308
Clarke D.A., Bridle A.H., Burns J.O., Perley R.A., Norman M.L., 1992, ApJ, 385, 173
Clarke D.A., Burns J.O., Norman M.L., 1992, ApJ, 395, 444
Franceschini A., Vercellone S., Fabian A.C., 1998, MNRAS, 297, 817
Gizani N.A.B., Leahy J.P., 2003, MNRAS, 342, 399
Guiderdoni B., Rocca-Volmerange B., 1987, A&A, 186, 1
Hardcastle M.J., Alexander P., Pooley G.G., Riley J.M., 1997, MNRAS, 288, 859
Ivezić Z., et al. 2002, AJ, 124, 2364
Ivezić Z., et al. 2004, ASPC, 311, 347
Jeyakumar S., Saikia D.J., 2000, MNRAS, 311, 397
Junkes N., Haynes R.F., Harnett J.I., Jauncey D.L., 1993, A&A, 269, 29
Kaiser C.R., Alexander P., 1997, MNRAS, 286, 215
Kaiser C.R., Schoenmakers A.P., Röttgering H.J.A., 2000, MNRAS, 315, 381
Komissarov S.S., Gubanov A.G., 1994, A&A, 285, 27
Kronberg P.P., Wielebinski R., Graham D.A. 1986, A&A, 169, 63
Leahy J.P., Perley R.A., 1991, AJ, 102, 537
Leahy J.P., Pooley G.G., Riley J.M., 1986, MNRAS, 222, 753
Leahy J.P., Black A.R.S., Dennett-Thorpe J., Hardcastle M.J., Komissarov S., Perley R.A., Riley J.M., Scheuer P.A.G., 1997, MNRAS, 291, 20
Loken C., Burns J.O., Clarke D.A., Norman M.L., 1992, ApJ, 392, 54
Marconi A., Risaliti G., Gilli R., Hunt L.K., Maiolino R., Salvati M., 2004, MNRAS, 351, 169
Marecki A., Barthel P.D., Polatidis A., Owsianik I., 2003, PASA, 20, 16
Miley G. K., 1980, ARA&A, 18, 165
Myers S. T., Spangler S. R., 1985, ApJ, 291, 52
Morganti R., Killeen N.E.B., Ekers R.D., Oosterloo T.A., 1999, MNRAS, 307, 750

Nipoti C., Blundell K.M., Binney J., 2005, MNRAS, 361, 633
Owen F.N., Ledlow M.J., 1997, ApJS, 108, 41
Padrielli L., Kapahi V.K., Katgert-Merkelijn J.K., 1981, A&AS, 46, 473
Perley R.A., Bridle A.H., Willis A.G., Fomalont E.B., 1980, AJ, 85, 499
Roettiger K., Burns J.O., Clarke D.A., Christiansen W.A., 1994, ApJ, 421, 23L
Saikia D.J., Thomasson P., Spencer R.E., Mantovani F., Salter C.J., Jeyakumar S., 2002, A&A, 391, 149
Saripalli L., Subrahmanyan R., Udaya Shankar N., 2002, ApJ, 565, 256
Saripalli L., Subrahmanyan R., Udaya Shankar N., 2003, ApJ, 590, 181
Schilizzi R.T. et al., 2001, A&A, 368, 398
Schoenmakers A.P., de Bruyn A.G., Röttgering H.J.A., van der Laan H., Kaiser C.R., 2000, MNRAS, 315, 371
Spergel D.N. et al., 2003, ApJS, 148, 175
Stanghellini C., O'Dea C.P., Dallacasa D., Cassaro P., Baum S.A., Fanti R., Fanti C., 2005, A&A, submitted, (astro-ph/0507499)
Strom R.G., Willis A.G., 1980, A&A, 85, 36
Subrahmanyan R., Saripalli L., Hunstead R.W., 1996, MNRAS, 279, 257
van Breugel W., Fomalont E.B., 1984, ApJ, 282, 55L
Willis A.G., Strom R.G., Wilson A.S., 1974, Nature, 250, 625